Chinese Journal of
POLYMER SCIENCE

RESEARCH ARTICLE

https://doi.org/10.1007/s10118-026-3886-0
Chinese J. Polym. Sci.

Scalable All-biomass Nanofibers: Energy-save Exfoliation and Application as Eco-friendly Functional Coatings

Yan Zhou[a,†], Zheng-Hao Xia[b,†], Jian-Zheng Yang[a], Chun-Chun Yin[b], Jiang-Hao Wen[a], Jin-Ming Zhang[b*], Hai Wang[a], and Jun Zhang[b*]

[a] *Center for Environmental Metrology, National Institute of Metrology, Beijing 100029, China*
[b] *CAS Key Laboratory of Engineering Plastics and CAS Research/Education Center for Excellence in Molecular Sciences, Institute of Chemistry, Chinese Academy of Sciences, Beijing 100190, China*

Electronic Supplementary Information

Abstract The preparation and application of biomass nanomaterials represent a crucial pathway for the high-value utilization of natural biomass resources. Developing simple and energy-saving strategies for converting biomass into all-biomass nanomaterials is fascinating and of practical value. Herein, we propose a simple and energy-saving method to fabricate all-biomass nanofibers (ANFs) using natural biomass, such as bamboo powder and straw. By removing part of the hemicellulose and lignin, the interactions between the nanofibers in natural biomass are disrupted, resulting in all-biomass micronanofibers. Subsequently, ANFs were obtained by ultrasonic oscillation. The entire process is simple and operates under mild conditions, eliminating the need for energy-intensive high-pressure homogenization or specialized equipment, thereby facilitating scalable production. This method preserves cellulose, along with most hemicellulose and lignin, thus achieving a high biomass utilization rate. Moreover, the retention of hemicellulose and lignin endows the obtained ANFs with desirable properties including ultraviolet resistance and high haze. ANFs can spontaneously form high-strength film and binder-free straws. Based on the nanoscale effect and excellent complete biodegradability, ANFs can be used as eco-friendly functional coatings for fruit and vegetable preservation, as well as high-throughput oil-water separation. Thus, this work not only provides an efficient and energy-saving method for preparing ANFs but also achieves the high-value utilization of low-grade biomass resources.

Keywords Biomass; Nanofibers; Lignocellulose; Fruit preservation; Oil-water separation

Citation: Zhou, Y.; Xia, Z. H.; Yang, J. Z.; Yin, C. C.; Wen, J. H.; Zhang, J. M.; Wang, H.; Zhang, J. Scalable all-biomass nanofibers: energy-save exfoliation and application as eco-friendly functional coatings. *Chinese J. Polym. Sci.* https://doi.org/10.1007/s10118-026-3886-0

INTRODUCTION

Plants exhibit highly complex compositions and hierarchical structures. They not only contain multiple components, including cellulose, hemicellulose, lignin, and inorganic salts, but also feature cellulose chains that form hierarchical aggregates *via* hydrogen-bonding interactions.[1–4] In higher plants, 36 cellulose chains self-assemble through interchain interactions to form nanoscale aggregated structures approximately 3–5 nm in diameter and exceeding 2 μm in length, known as cellulose nanofibers (CNFs).[5] These CNFs further aggregate and assemble into cellulose microfibrils with diameters of 10–40 nm, which are typically encapsulated by hemicellulose and lignin. Through an ordered arrangement, the cellulose microfibrils ultimately assemble into cellulose macrofibrils with diameters of approximately 100 nm. The unique multilevel micro-nano structure of natural biomass lays the foundation for fabricating high-performance biomass nanomaterials, such as cellulose nanocrystals (CNCs) and CNFs.[6–10] Specifically, by selectively removing the amorphous regions of cellulose while preserving its crystalline domains, nanomaterials with diameters of approximately 5–20 nm and lengths ranging from 50 nm to 600 nm can be obtained, which are defined as CNCs. Conversely, if the amorphous regions were retained and only the nanofibers were separated, the resulting materials would be CNFs. Both CNCs and CNFs have distinctive nanostructures, exceptional mechanical and thermal stability, and excellent biocompatibility, enabling their wide-ranging applications in fields such as optoelectronics, biomedicine, and energy storage/conversion.[11–16] However, the current preparation methods for CNCs are plagued by low yields, whereas those for CNFs involve enormous energy consumption. These issues severely hinder the practical applications of CNCs and CNFs. In recent years, novel methods for preparing nanocellulose have been developed, including deep eutectic solvents (DES), chemical-mechanical synergistic, and biosynthetic methods. For example, Liu *et al.* employed a DES/acidic solvent system to swell cellulose, followed by esterification.[17] Following this treatment, high-pressure ho-

* Corresponding authors, E-mail: zhjm@iccas.ac.cn (J.M.Z.)
E-mail: jzhang@iccas.ac.cn (J.Z.)
† These authors contributed equally to this work.
Received July 21, 2026; Accepted September 11, 2026; Published online November 13, 2026

© Chinese Chemical Society
Institute of Chemistry, Chinese Academy of Sciences

mogenization, which is characterized by high energy consumption, was employed to isolate cellulose; thus, CNFs with diameters of 20–40 nm were fabricated with a yield of 72%–88%. Zhou *et al.* dispersed cellulose in a LiOH/DMSO quasi-solvent system under intense stirring to selectively disrupt the hydrogen bonding and van der Waals forces between elementary cellulose fibrils, resulting in a highly swollen network.[18] Cyclic acid anhydride was then added for esterification, followed by treatment with ethanol and an aqueous NaOH solution. Finally, through time-consuming processes including stirring, centrifugation, and dialysis, a CNFs suspension with an ultrahigh aspect ratio (approximately 1400) was prepared. Yang *et al.* performed surface cationization of cellulose using 2,3-epoxypropyltrimethylammonium chloride, followed by intensive mechanical exfoliation, which resulted in the preparation of lignocellulosic microfibers, nanofibers, and two-dimensional sheet materials.[19] Similarly, Sirviö *et al.* adopted a cationization strategy using wood chips as the raw material.[20] Lignocellulosic nanofibers (LCNFs) were obtained by cationization and mechanical pulverization in a tetraethylammonium hydroxide/urea/glycidyl trimethylammonium chloride solvent system. Yang *et al.* used spruce as a raw material and selectively removed lignin *via* a peracetic acid treatment.[21] Following NaOH washing, vigorous mechanical stripping, and centrifugal purification, ultrafine holocellulose nanofibers (Holo-CNFs) with a diameter of <5 nm that retained natural structural features were successfully obtained, achieving a yield of approximately 27%. Yu *et al.* pretreated poplar chips using choline chloride/oxalic acid/ethylene glycol as solvents to remove most hemicellulose and lignin.[22] Ultra-high-speed mechanical defibrillation was adopted to prepare LCNFs with a minimal lignin content. The preparation of nanocellulose typically requires intensive mechanical processes, such as high-pressure homogenization, grinding treatment, and chemical modification, followed by prolonged purification to disrupt the interactions between the nanofibers. These processes are characterized by high energy consumption, time-consuming operation, and susceptibility to equipment clogging. Furthermore, the production of both CNCs and CNFs usually requires high-purity cellulose feedstock, which requires nearly complete removal of hemicellulose and lignin. Such approaches often result in underutilization of biomass resources and contribute to environmental pollution. Existing nanocellulose preparation technologies generally suffer from the following issues: (1) high requirements for raw material purity and complex pretreatment processes; (2) stringent equipment specifications and high energy consumption; and (3) long processing duration, low production efficiency, and limitations to large-scale manufacturing. Therefore, the development of efficient, energy-saving, and readily scalable strategies for preparing biomass nanofibers is of considerable scientific importance and practical value.[23–25]

In this study, a simple, energy-saving, and scalable strategy was demonstrated to directly fabricate all-biomass nanofibers (ANFs) from natural biomass (Fig. 1). It involves the partial removal of hemicellulose and lignin to disrupt the interactions between natural nanofibers, followed by ultrasonic oscillation. The entire process is facile, scalable, rapid, and energy saving. Furthermore, cellulose, along with most hemicellulose and lignin, is retained during preparation, thus achieving a high biomass utilization rate. The resulting ANFs can serve as fully biodegradable functional coatings for fruit and vegetable preservation, as well as oil-water separation (Fig. 1).

EXPERIMENTAL

Materials

Bamboo and wheat straw were purchased from Jiangsu Lianfeng Agricultural Products Processing Co., Ltd., and *p*-tosyl sulfonic acid (*p*-TsOH), ethylene glycol (EG), and 1,4-butanediol (BDO) were purchased from Innochem Chemical Reagents Co., Ltd. Isooctane, *n*-hexadecane, silicone oil, and tween-80 were purchased from J&K Scientific Co., Ltd. The soybean oil used was an Arowana-blended cooking oil.

Preparation of All-biomass Nanofibers

The bamboo powder, sieved through an 80-mesh screen, was added to a 2% NaOH solution to prepare a slurry with a solid content of 10%. After stirring at 60 °C for 0.5 h, the mixture was centrifuged and washed until neutral pH was achieved. It was then added to the *p*-TsOH/H_2O, *p*-TsOH/EG, or *p*-TsOH/BDO solvent systems (mass ratio of *p*-TsOH to cosolvent = 8:2) at a solid content of 10%, followed by stirring at 80 °C for 20 min. An appropriate amount of water was then added to terminate the reaction. The mixture was centrifuged, washed several times with ethanol, and then sequentially washed with deionized water and dried to obtain all biomass micro-nanofibers. These micro-nanofibers were dispersed in deionized water at concentrations of 0.3%, 0.5%, and 1% and sonicated in a cell disruptor at 400 W for 30 min to yield ANFs. The yield of ANFs was calculated based on the dry mass of the final ANFs relative to that of the initial dry raw material. The calculation formula is as follows:

$$\text{Yield}\,(\%) = \frac{m_{\text{ANFs(dry)}}}{m_{\text{raw material (dry)}}} \times 100 \quad (1)$$

where $m_{\text{ANFs(dry)}}$ are the dry masses of ANFs, $m_{\text{raw material (dry)}}$ represents the dry mass of the initial raw material.

Preparation of Fruit Preservation Coatings

The ANFs aqueous dispersion with a solid content of 0.5%–1.0% was sprayed onto the banana surface. After the surface was dried, it was sprayed again and dried to ensure that the entire banana surface was fully covered with ANFs. The decay status of the banana surface was observed daily and the bananas were weighed to evaluate their degree of decay.

Preparation of Oil-water Separation Membrane

A nonwoven cellulose fabric was used as the substrate. The nonwoven fabric was placed in a solvent filter and the ANFs aqueous dispersion was poured into it. ANFs/cellulose oil-water separation membranes were prepared with ANFs deposition densities of 4.08, 7.13, and 10.19 g/m^2, which were used for emulsion oil-water separation.

Four types of oils (isooctane, *n*-hexadecane, silicone oil, and edible oil) were individually mixed with deionized water in a volume ratio of 2:98, with a total volume of 200 mL. After adding 0.4 g of Tween-80, the mixture was magnetically stirred for 6 h to obtain oil-water emulsions.[26] The four oil-water emulsions were poured into a solvent filter with an ANF/cellulose oil-water separation membrane clamped inside, followed by vacuum filtration. The filtrate was collected, oil content was measured, and separation time was recorded.

The emulsion separation efficiency of the ANF/cellulose oil-water separation membranes was calculated using the following formula:

https://doi.org/10.1007/s10118-026-3886-0

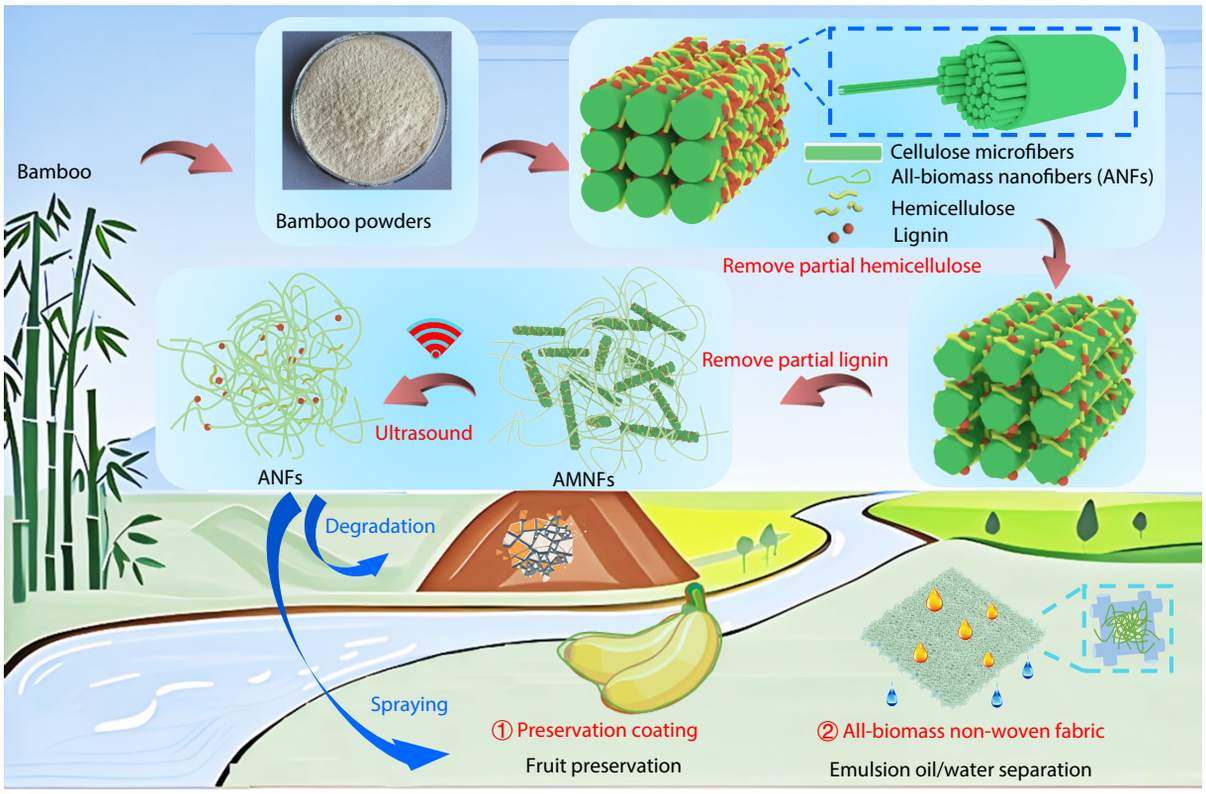


Fig. 1 Schematic diagram of the preparation and application of ANFs.

$$\text{Separation efficiency (\%)} = \left(1 - \frac{C_2}{C_1}\right) \times 100 \quad (2)$$

where C_1 and C_2 represent the oil concentration in water before and after oil-water separation, respectively. Both values were measured using an infrared oil content analyzer (OIL480, China).

The separation flux F (L/(m^2·h)) of the ANF/cellulose oil-water separation membranes was calculated according to the following formula:

$$F = \frac{V}{S \times t} \quad (3)$$

where V is the volume of the mixture, S is the area of the separation membrane, and t is the separation time.

Characterization

The contents of cellulose, hemicellulose, and lignin in the biomass were determined following the method for carbohydrate and lignin content analysis in biomass from the National Renewable Energy Laboratory (NREL, USA). Lignin removal was photographed using an inverted fluorescence microscope (Olympus IX71, Japan). The microscopic morphology of the ANFs was observed *via* scanning electron microscopy (Hitachi S8020, Japan), transmission electron microscopy (JEOL-1011, Japan), and atomic force microscopy (Multimode 8, Bruker, Germany). For TEM sample preparation, the ANFs aqueous dispersion was diluted, dropped onto a carbon-supported film, and air-dried. Mechanical properties were tested using a universal testing machine (Instron 3365, INSTRON, USA) at a tensile rate of 5 mm/min. The average values and standard deviations were calculated from at least five replicate measurements.

XRD patterns were recorded on an X-ray diffractometer (Panalytical B.V. Empyrean, Netherlands) in reflection mode over a 2θ range of 5°–60° at a scanning rate of 2 (°)/min. Fourier transform infrared (FTIR) spectra were obtained using a Nicolet 6700 FTIR spectrometer (Thermo Fisher, USA) with a resolution of 0.125 cm^{-1} by accumulating 64 scans. Thermal stability tests were performed using a thermogravimetric analyzer (TGA 8000, PerkinElmer, USA) under a nitrogen atmosphere at a heating rate of 20 °C/min over a temperature range of 50–750 °C. The emulsion preparation process and the liquids after oil-water separation were observed using a Leica DMLP polarizing microscope (Leica Company, Germany). The underwater contact angles were determined using a video-based contact angle measurement system (OCA 40, Data-physics, Germany), where the volume of each oil droplet was 10 μL.

RESULTS AND DISCUSSION

Fabrication of All-biomass Nanofibers

Natural biomass is composed primarily of cellulose, hemicellulose, and lignin. These components exhibit strong interactions, forming a robust biomass recalcitrance structure that resists disruption, which hinders the separation and utilization of natural biomass. Hemicellulose and lignin act as adhesives, playing a crucial role in the formation of the biomass recalcitrance structure. Thus, hemicellulose was partially removed using 2% NaOH at 60 °C, followed by partial lignin removal using *p*-tosyl sulfonic acid (*p*-TsOH). These treatments partially eliminated the adhesive layer between the cellulose nanofibers, and the subsequent ultrasonic oscillation yielded ANFs (Fig. 1). Bamboo powder (BP) was used as the model to verify the preparation protocol. Bamboo powder, a byproduct of bamboo processing, is an

agricultural and forestry waste material. SEM observation revealed that the green bamboo powder, following treatment with NaOH and *p*-TsOH, changed from its initial short rod-shaped microparticles to microfibers and nanofibers (Fig. 2a). Subsequent ultrasonication facilitated almost complete conversion to nanofibers. These findings confirm that ANFs can be successfully preparation of ANFs from natural biomass materials *via* the partial removal of lignin and hemicellulose.

Treatment of biomass feedstock with 2% NaOH at 60 °C for 0.5 h effectively removed part of the hemicellulose and lignin.

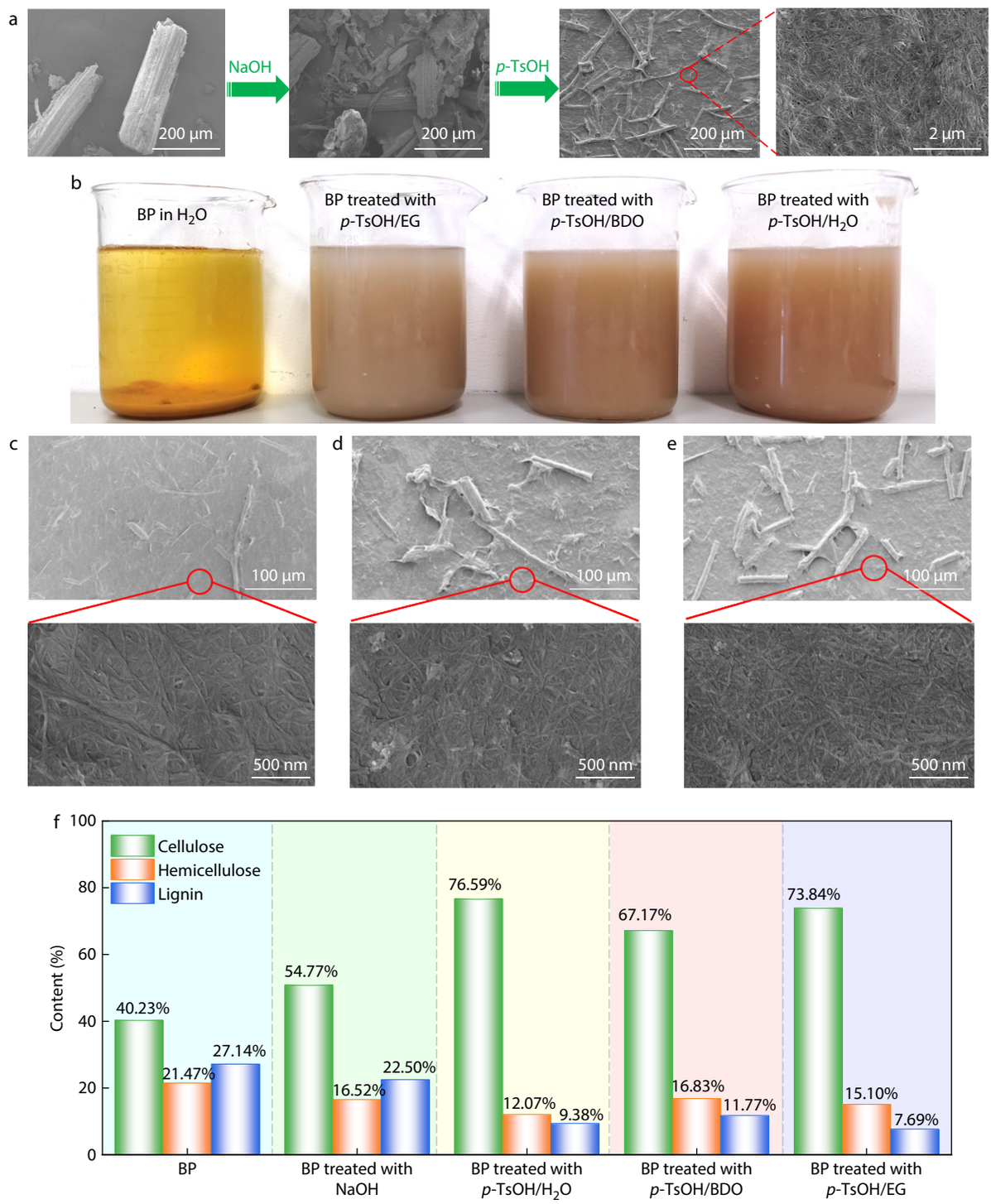


Fig. 2 Morphology and compositions of bamboo powder after sequential NaOH and *p*-TsOH treatments. (a) SEM images of bamboo powder before and after NaOH and *p*-TsOH treatment; (b) Optical photographs of bamboo powder before and after *p*-TsOH/EG, *p*-TsOH/BDO, and *p*-TsOH/H_2O treatments; (c–e) SEM images of bamboo powders treated with (c) *p*-TsOH/EG, (d) *p*-TsOH/BDO, and (e) *p*-TsOH/H_2O, respectively; (f) Contents of cellulose, hemicellulose, and lignin in pure and treated BP.

https://doi.org/10.1007/s10118-026-3886-0

After treatment, the hemicellulose content decreased from 21.47% to 16.52%, and the lignin content decreased from 27.14% to 22.50% (Fig. 2f). At this stage, the bamboo powder failed to disperse in the water and rapidly sank to the bottom (Fig. 2b). The bamboo powder was further treated with a mixture of *p*-TsOH/H_2O, *p*-TsOH/1,4-butanediol (BDO), or *p*-TsOH/ethylene glycol (EG) to remove additional lignin, resulting in a lignin content of less than 12% (Fig. 2f). Subsequently, the green bamboo powder could suspend and disperse in water, forming all-biomass micro- and nanofibers (AMNFs) (Figs. 2b–2e).

The preparation process of ANFs were prepared from bamboo powder and observed using fluorescence microscopy (Fig. 3a). With *p*-TsOH/H_2O as the solvent, most of the lignin (green fluorescence) in the bamboo powder was rapidly removed within 30 s. For the bamboo powder with higher biorecalcitrance, lignin could also be removed within 600 s (Fig. S1 in the electronic supplementary information, ESI). The sequential removal of partial hemicellulose and partial lignin enabled the successful preparation of AMNFs (Fig. 3b). After ultrasonic agitation of the resulting AMNFs for 15 min, nearly all microfibers were exfoliated into nanofibers (Fig. 3c). The solid content of the AMNFs aqueous dispersions was controlled at 0.3%, 0.5%, and 1%. Among them, the dispersion with a solid content of 0.3% exhibited the best exfoliation effect, being composed entirely of nanofibers (Fig. 3d), whereas samples with solid contents of 0.5% and 1% still contained small quantities of microfibers (Figs. 3e and 3f). The nanofibers obtained were entangled with each other, forming a network structure. Atomic force microscopy (AFM) analysis revealed that the ANFs in the dispersion with a 0.3% solid content exhibited the smallest fiber diameter, approximately 32.2 nm (Fig. S2 in ESI). As the solids content increased, the diameter of the ANFs gradually increased. For the sample with a solids content of 1%, the nanofiber diameter increased to 47.0 nm. The yield of the ANFs was calculated to be 51.8% by comparing their mass with that of the initial raw material.

To verify the universality of this method, wheat straw, a common agricultural waste, was used as raw material. After sequential treatment with NaOH and *p*-TsOH/H_2O, followed by ultrasonic exfoliation, ANFs were successfully fabricated (Fig. S3 in ESI). The pretreated wheat straw powder was ultrasonicated for 30 min to achieve an almost complete conversion into nanofibers. Owing to the high content of impurities in wheat straw, some nanoparticles were present in the resulting nanofibers, and their aqueous suspension appeared brown (Fig. S4 in ESI). This method demonstrates excellent universality and is applicable to various lignocellulosic biomass feedstock. Moreover, the preparation process is readily scalable for industrial production, eliminating the need for an energy-intensive homogenization step.

Formability and Degradability of AMNFs and ANFs

After vacuum filtration and drying, the AMNFs and ANFs yielded yellow or brown translucent paper (Figs. 4a and 4b). Prior to drying, the papers were curled without binders, resulting in a fully biomass-derived straw after drying (Fig. 4c). The incorporation of both microscale and nanoscale fibers generated an all-biomass paper characterized by a highly undulating surface with a pleated morphology (Fig. S5 in ESI), featuring an uneven cross-section with numerous defects. In contrast, the ANFs paper displayed a smooth surface and cross section (Fig. S5 in ESI). Both the AMNFs and ANFs papers exhibited excellent mechanical properties. The tensile strength of AMNFs paper reaches (80.4±4.6) MPa, and that of ANFs paper achieves (100.9±10.8) MPa (Fig. 4d). The AMNFs and ANFs papers exhibited high visible light transmittance, exceeding 60.1% and 80.8%, respectively, at 800 nm (Fig. 4e). In addition, the retention of hemicellulose (indicated by the C=O stretching vibration at 1728 cm^{-1}) and lignin (evidenced by the benzene ring C—H stretching vibrations between 1400–1600 cm^{-1}) endows the resulting AMNFs and ANFs papers with ultraviolet resistance and high haze (Fig. S6 in ESI). Notably, the AMNFs paper exhibited a high haze of up to 94.4% in the visible region (Fig. 4f). XRD analysis confirmed that cellulose I crystallinity was consistently present in the original bamboo powder, AMNFs, and ANFs paper (Fig. S7 in ESI). TGA analysis indicated a higher thermal stability of ANFs compared to that of AMNFs (Fig. S8 in ESI).

The prepared AMNFs paper and straw consisted of natural cellulose, lignin, and hemicellulose, and thus exhibited excellent biodegradability. Under composting conditions, AMNFs straw fully degraded within eight days, whereas AMNFs paper degraded completely within six days (Figs. 4g and 4h).

Application of ANFs

The ANFs coating was constructed on banana surfaces *via* spraying a ANFs aqueous dispersion of ANF (Fig. 5a). ANFs coating improved fruit preservation. The coated bananas consistently exhibited lower weight loss percentages than the untreated bananas throughout the storage period (Fig. 5b). After 7 days of storage, epidermal browning was markedly suppressed in coated bananas (Figs. 5c and 5d), confirming that the coating prolonged shelf life. These good preservation properties stem from the high barrier performance of ANFs coatings. Moreover, the dense network structure of the ANFs coating retarded water loss. This impedes oxygen permeation also,[27–29] thereby delaying the oxidative and deterioration processes of the fruits. Thus, the biodegradable ANFs coating demonstrated potential as an eco-friendly disposable preservation material, providing a sustainable strategy for extending the shelf life of fruits.

An all-biomass-based oil-water emulsion separation membrane (AESM) was fabricated on a cellulose nonwoven substrate featuring microfibers approximately 10 μm in diameter *via* uniform deposition of a 1% solid-content ANFs aqueous dispersion. The areal density of the deposited nanofibers was controlled at 7.13 g/m^2 (Fig. 6a). SEM images indicate that the ANFs self-assembled on the substrate surface, forming a separation layer with a micro-nano hierarchical architecture (Fig. 6b). Owing to its excellent hydrophilicity and unique microstructure, the membrane exhibits high water permeability while effectively blocking the oil phase, thus enabling highly selective and efficient oil-water separation. Four typical oils, soybean oil, silicone oil, isooctane, and n-hexadecane, were selected, and white emulsions were prepared by adding the surfactant Tween-80 followed by stirring for 6 h (Fig. 6c). Contact angle measurements revealed that the underwater oil contact angles of the membranes for all four oils exceeded 130° (Fig. 6d), demonstrating pronounced underwater oleophobicity. This characteristic prevents oil droplets from spreading on the membrane surface, thereby ensuring the ef-

https://doi.org/10.1007/s10118-026-3886-0

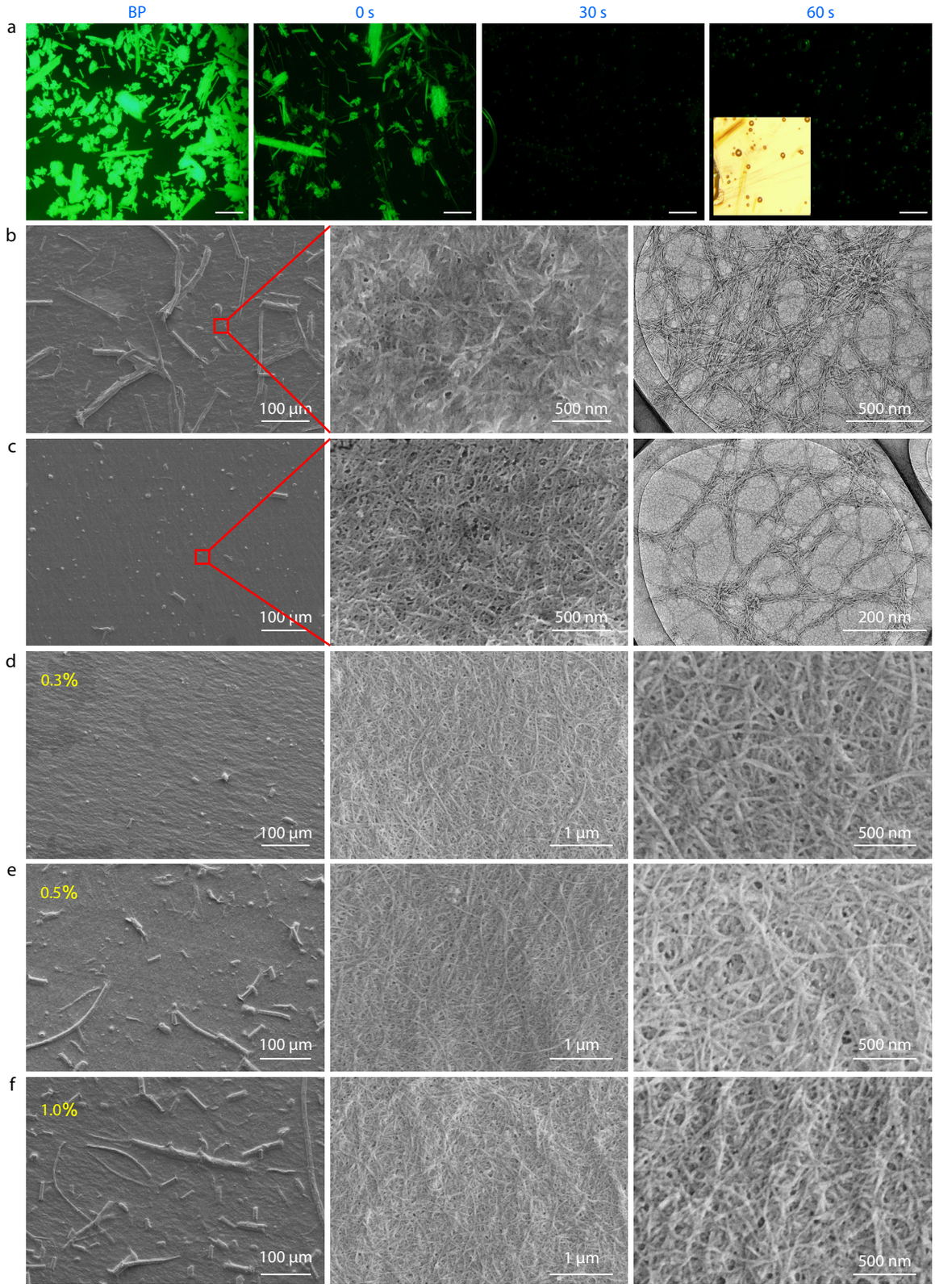


Fig. 3 Preparation and morphological characterization of ANFs. (a) Lignin removal process of bamboo powder in *p*-TsOH/water system under fluorescence microscopy (scale bar: 100 μm); (b) SEM and TEM images of bamboo powder treated with NaOH and *p*-TsOH/EG system; (c) SEM and TEM images of ANFs; (d–f) Morphological characterization of ANFs dispersions with solid contents of (d) 0.3%, (e) 0.5%, and (f) 1%, respectively.

https://doi.org/10.1007/s10118-026-3886-0

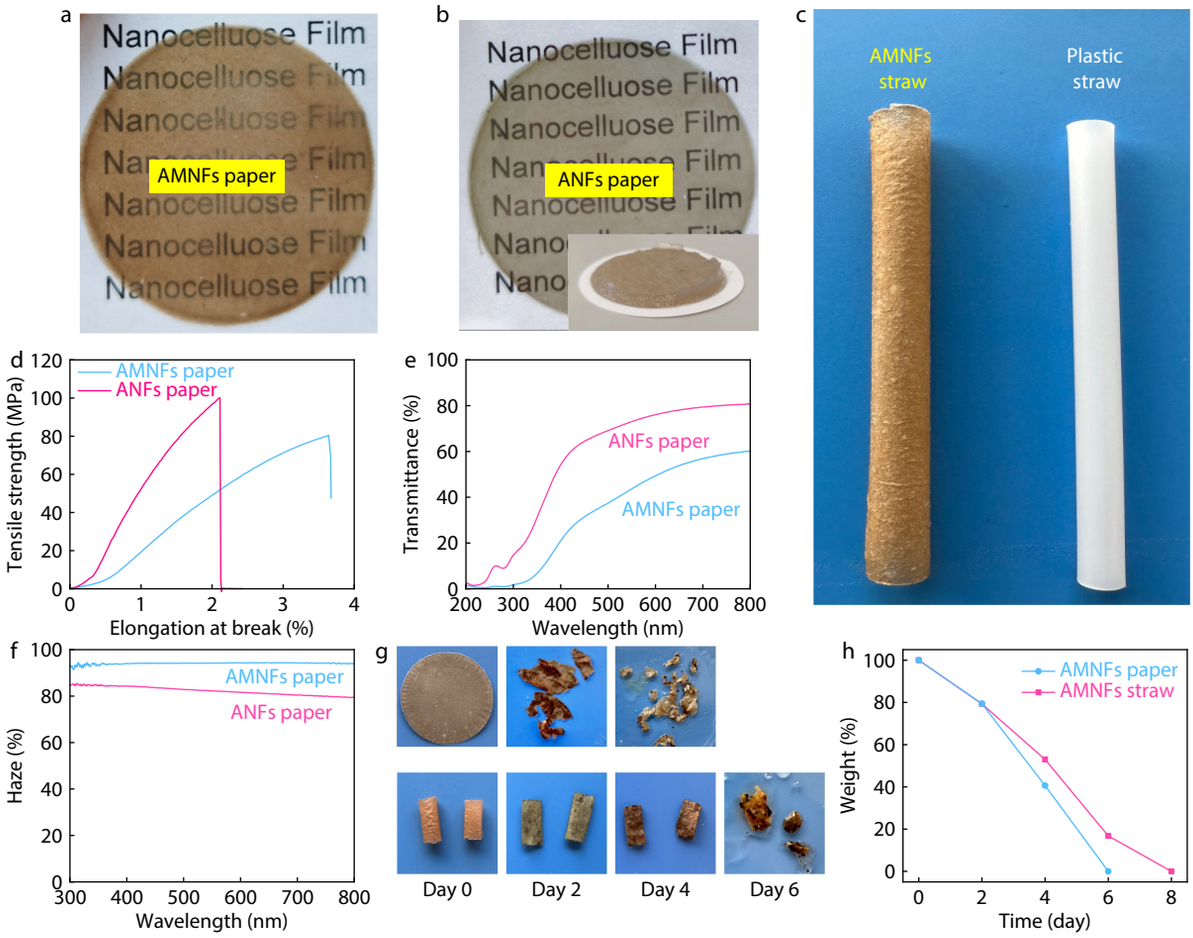
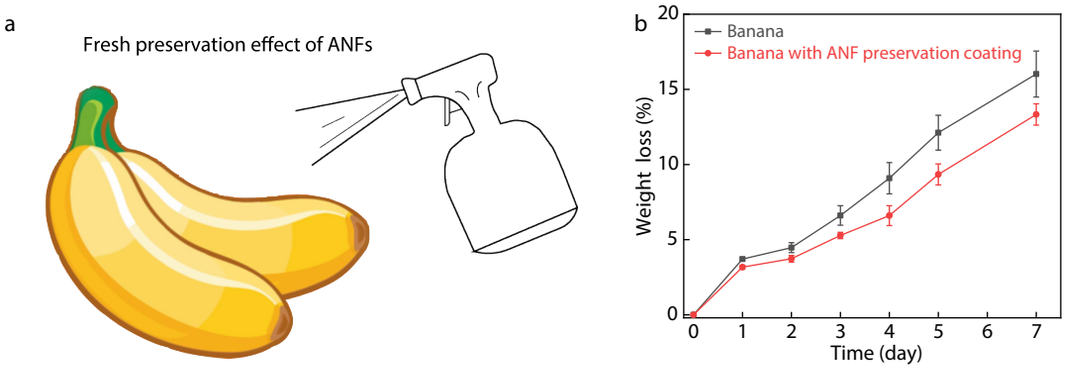


Fig. 4 Formability and degradability of AMNFs and ANFs. Optical photographs of (a) AMNFs paper, (b) ANFs paper, and (c) AMNFs straw and plastic straw; (d) Mechanical properties, (e) light transmittance, and (f) haze of AMNFs and ANFs papers; (g) Photographs of the degradation process and (h) weight loss curves of AMNFs straw and paper.

fective retention of the oil phase in the upper layer of the membrane during separation.

The oil-water separation capability of the fabricated membrane was assessed *via* a filtration-based approach (Fig. S9 in ESI). Optical microscopy observations demonstrated that the effluent treated by the oil-water separation membrane was clear and transparent, with no residual oil droplets detected (Fig. 6e). Notably, the membrane achieved an oil-water separation efficiency exceeding 99.59% for emulsions formulated with four distinct types of oils (Fig. 6f). The separation flux is influenced by the oil viscosity. Silicone oil, with a higher viscosity, showed a lower flux of approximately 458 L/(m^2·h), whereas *n*-hexadecane, with a lower viscosity, achieved a higher flux of approximately 1091 L/(m^2·h). To further explore the tunability of the biomass-derived separation membrane, ANFs coatings were applied to cellulose nonwoven substrates at surface densities of 4.08, 7.13, and 10.19 g/m^2. With an increase in areal density, the compactness of the ANFs coating was gradually enhanced (Fig. S10 in ESI), which led to a progressive decrease in the separation flux under con-



https://doi.org/10.1007/s10118-026-3886-0

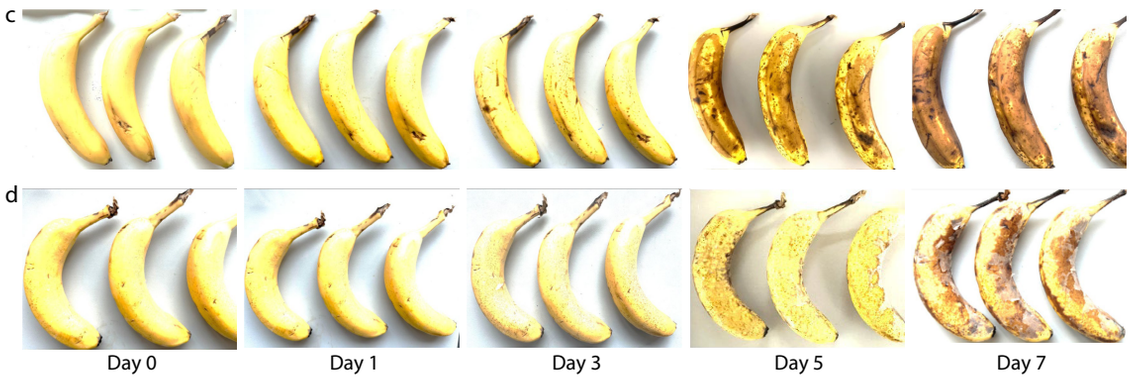
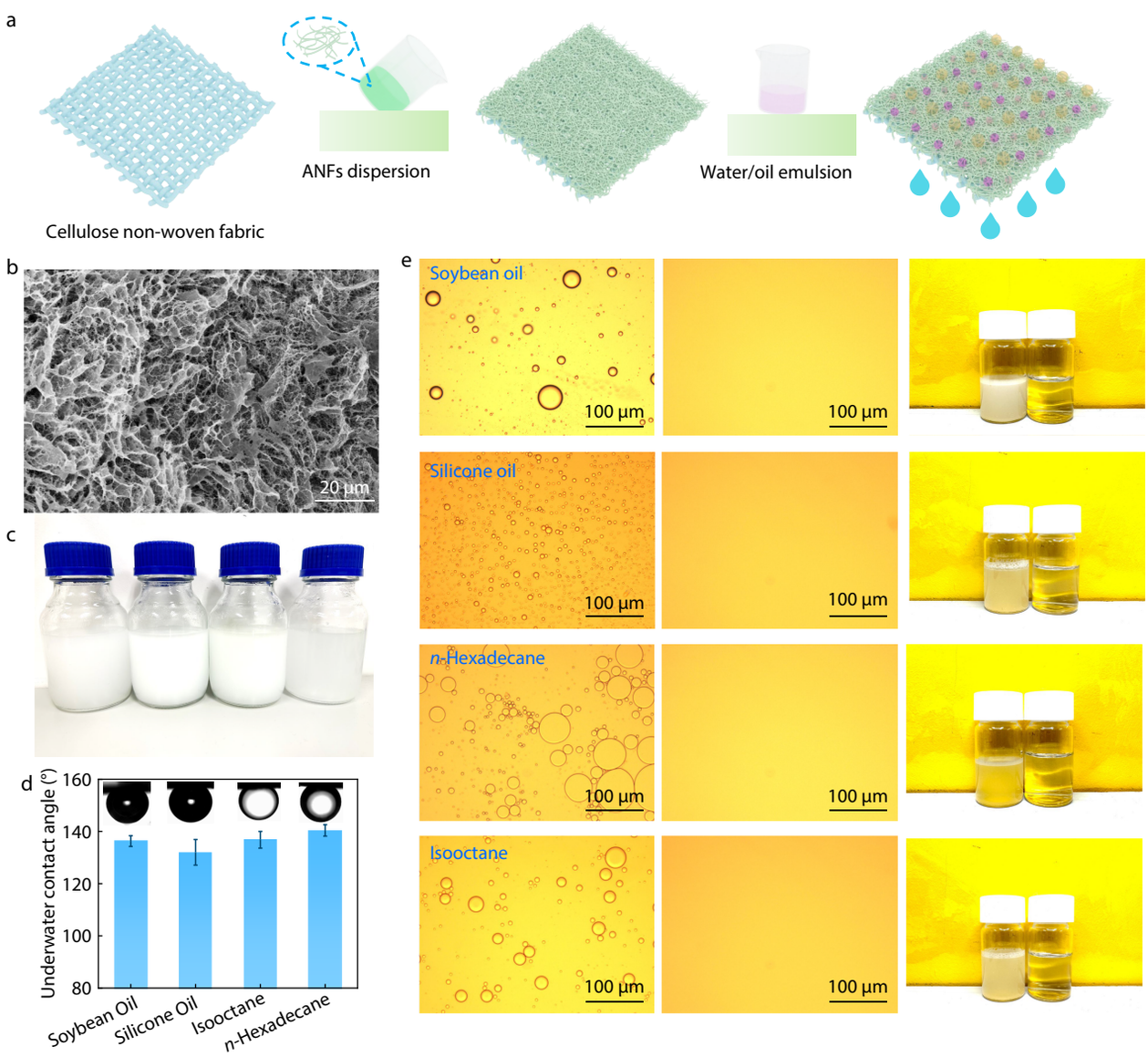


Fig. 5 Preservation effect of ANFs coating on fruits. (a) Schematic diagram of ANFs for fruit preservation; (b) Weight loss curves of uncoated and ANFs-coated bananas; Rotting conditions of bananas (c) without and (d) with ANFs coating.

stant pressure (Fig. 6g). Even at a reduced areal density of 4.08 g/m^2, the separation membrane maintained a high oil-water separation efficiency (>99.5%) along with enhanced separation flux (Fig. 6h). These findings demonstrate that the separation performance of an all-biomass separation membrane can be precisely modulated *via* the areal density of the



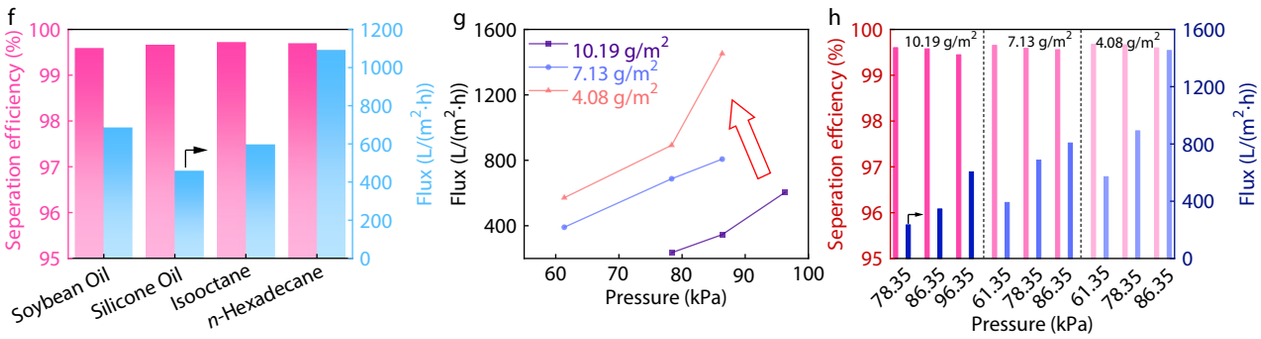


Fig. 6 Oil-water separation performance of ANFs/cellulose membranes. (a) Schematic illustration of the fabrication process for the all-biomass emulsion oil-water separation membrane; (b) SEM image of the separation layer of the emulsion oil-water separation membrane; (c) Photographs of emulsions containing soybean oil, silicone oil, isooctane, and *n*-hexadecane; (d) Underwater contact angles of four oils on the separation membrane; (e) Optical microscopy images and photographs of emulsions before and after separation; (f) Emulsion separation efficiency and flux; (g) Variation curve of emulsion separation flux of the membrane with different areal densities; (h) Separation efficiency and flux of the membrane under different pressures and areal densities.

coating. It achieves an ultrahigh separation efficiency while enabling tailored flux performance to meet specific practical requirements. This adaptability confers substantial application potential to the membrane in the treatment of oil-water systems with varying viscosities.

CONCLUSIONS

In this study, a scalable and energy-saving strategy for the fabrication of all-biomass nanofibers (ANFs) is proposed. Natural bamboo powder and straw were employed as raw materials, with partial removal of hemicellulose and lignin to disrupt the intrinsic interactions between nanofibers in the natural biomass, thereby yielding AMNFs. Subsequently, the microfibers were exfoliated *via* ultrasonic oscillation to obtain ANFs. The hemicellulose and lignin removal process is mild and simple, whereas the exfoliation step obviates the need for high-energy-consuming equipment, thus enabling scalable production. Affected by the treatment conditions and raw materials used, the resulting ANFs exhibited diameters ranging from 30 nm to 50 nm. Given that cellulose, partial hemicellulose, and lignin are all retained within ANFs, the utilization efficiency of biomass resources is substantially improved. Moreover, the resulting AMNFs exhibited advantages such as UV resistance, high haze, excellent mechanical strength, and complete biodegradability. ANFs readily form dense coatings that prevent moisture loss and oxygen permeation, thus making them suitable for fruit and vegetable preservation. Additionally, ANFs can be structured into micro/nanoporous architectures, achieving efficient oil-water emulsion separation with high selectivity (>99.59%) and high flux (>1000 L/(m^2·h)). After use, ANFs can be discarded following simple cleaning and undergo complete degradation in natural environments. Thus, this work not only develops an efficient and energy-saving fabrication method for ANFs but also realizes the high-value conversion of low-quality biomass resources, which holds substantial application prospects in fields such as green packaging and environmental remediation.

Conflict of Interests

The authors declare no interest conflict.

Electronic Supplementary Information

Electronic supplementary information (ESI) is available free of charge in the online version of this article at http://doi.org/10.1007/s10118-026-3886-0.

Data Availability Statement

The related data of this study can be obtained from the author for reasonable reasons.

ACKNOWLEDGMENTS

This work was financially supported by the Key R&D Program of Shandong Province, China (No. 2025CXGC010508), the National Natural Science Foundation of China (Nos. 52603197 and 52573239), Center for Carbon Neutral Chemistry, ICCAS (No. CCNC-202402), and Special Projects for Basic Research of the Chinese Central Research Institutes (No. AKYZZ2647).

REFERENCES

1 Bhattarai, M.; Al-Terke, H.; Liu, K.; Wan, Z. M.; Kilpelaeinen, P.; King, A. W. T.; Khakalo, A.; Xu, J. Y.; Xu, C. L.; Ras, R. H. A.; Mattos, B. D.; Rojas, O. J. Wood biomolecules as agricultural adjuvants for effective suppression of droplet rebound from plant foliage. *Adv. Sci.* **2025**, *12*, 2416686 .

2 Snyder, P. J.; Allard, V.; Bhagia, S.; Farahi, R. H.; Lereu, A. L.; Backlund, M. P.; Passian, A. Hemicellulose modulates nanoscale lignin architecture in synthetic plant cell walls. *ACS Nano* **2025**, *19*, 40364−40382.

3 Zheng, S. S.; Sun, S. L.; Manker, L. P.; Luterbacher, J. S. Aldehyde-stabilization strategies for building biobased consumer products around intact lignocellulosic structures. *Acc. Chem. Res.* **2025**, *58*, 877−892.

4 Zhang, W. M.; Niu, W. T.; Tan, F. F.; Li, Y. Selective transformation of biomass and the derivatives for aryl compounds and hydrogen *via* visible-light-induced radicals. *Acc. Chem. Res.* **2025**, *58*, 1407−1423.

5 Xu, J. H.; Zou, Y. J.; Chen, H. J. Y.; Wan, Z. M.; Takagi, A.; Wang, Z. G.; Yu, J.; Liu, L.; Lu, Y.; Fan, Y. M.; Rojas, O. J. Magnetoresponsive cellulose nanofiber hydrogels: dynamic structuring, selective

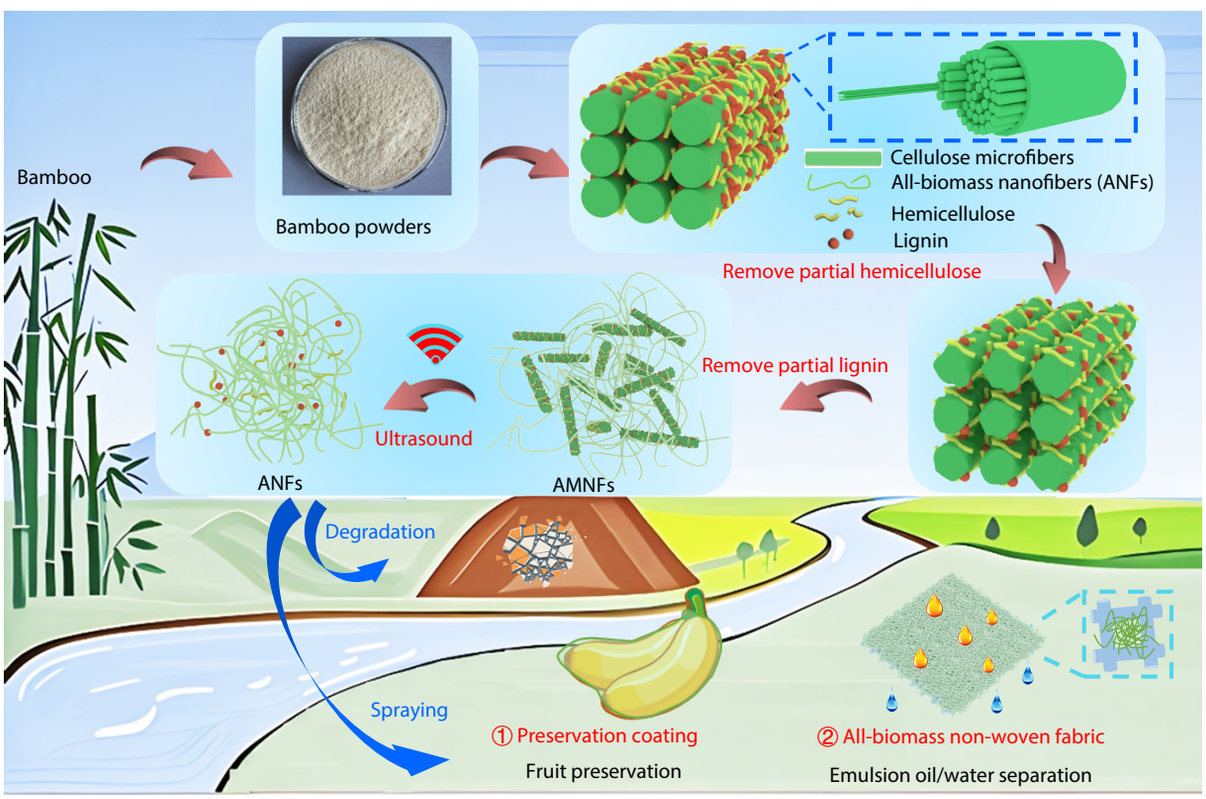
Graphical Abstract

Scalable All-biomass Nanofibers: Energy-save Exfoliation and Application as Eco-friendly Functional Coatings

Yan Zhou, Zheng-Hao Xia, Jian-Zheng Yang, Chun-Chun Yin, Jiang-Hao Wen, Jin-Ming Zhang, Hai Wang, and Jun Zhang

National Institute of Metrology; Institute of Chemistry, Chinese Academy of Sciences

Scalable all-biomass nanofibers were fabricated from natural biomass *via* the partial removal of hemicellulose and lignin, followed by ultrasonication. Biodegradable all-biomass nanofibers (ANFs) serve as eco-friendly coatings for fruit preservation and high-efficiency oil-water emulsion separation.



Chinese J. Polym. Sci. 2026 *https://doi.org/10.1007/s10118-026-3886-0*

light transmission, and information encoding. *ACS Nano* **2025**, *19*, 14063−14072.

6 Li, K.; Clarkson, C. M.; Wang, L.; Liu, Y.; Lamm, M.; Pang, Z. Q.; Zhou, Y. B.; Qian, J.; Tajvidi, M.; Gardner, D. J.; Tekinalp, H.; Hu, L. B.; Li, T.; Ragauskas, A. J.; Youngblood, J. P.; Ozcan, S. Alignment of cellulose nanofibers: harnessing nanoscale properties to macroscale benefits. *ACS Nano* **2021**, *15*, 3646−3673.

7 Habibi, Y. Key Advances in the chemical modification of nanocelluloses. *Chem. Soc. Rev.* **2014**, *43*, 1519−1542.

8 Li, Z. H.; Chen, C. J.; Xie, H.; Yao, Y.; Zhang, X.; Brozena, A.; Li, J. G.; Ding, Y.; Zhao, X. P.; Hong, M.; Qiao, H. Y.; Smith, L. M.; Pan, X. J.; Briber, R.; Shi, S. Q.; Hu, L. B. Sustainable high-strength macrofibres extracted from natural bamboo. *Nat. Sustain.* **2022**, *5*, 235−244.

9 Li, D. H.; Han, Z. M.; Shao, M.; Jiao, Z. J.; Gao, C.; Sun, W. B.; Liu, Z. X.; Yang, K. P.; Guan, Q. F.; Yu, S. H. A robust, biodegradable, and fire-retardant cellulose nanofibers-based structural material fabricated from natural sargassum. *Adv. Mater.* **2025**, *37*, 2417617.

10 Ke, Q. F.; Qin, Z. Y.; Zhang, Y. F.; Yang, Y. X.; Zhang, Y. C.; Kou, X. R. Tunable mechanical properties of aroma microcapsules achieved *via* cellulose nanocrystals interfacial self-assembly strategies. *Carbohyd. Polym.* **2025**, *368*, 124252.

11 Parthasarathy, V.; Kumar, P. S.; Albert, A. A.; Krishnasamy, S.; Chandrasekar, M. Recent progress in nanocellulose-based biocomposites for bone tissue engineering and wound healing applications. *Carbohyd. Polym.* **2025**, *357*, 123455.

12 Yang, H. B.; Yue, X.; Liu, Z. X.; Guan, Q. F.; Yu, S. H. Emerging sustainable structural materials by assembling cellulose nanofibers. *Adv. Mater.* **2025**, *37*, 2413564.

13 Mao, Y. S.; Sheng, Y. H.; Fan, Z. Y.; Yang, J.; Liu, J.; Tang, C. X.; Fu, S. H. Atmospheric pressure dried discontinuous pore gradient structured CNF-based aerogel for ultra-low reflection, broadband, and super-high EMI shielding. *Adv. Funct. Mater.* **2025**, *35*, 2421492.
14 Chen, L. X.; Wang, X.; Zhuo, H. L.; Yin, C. C.; Luo, Q.; Zhang, J.; Zhang, J. M. Functional pharmaceutical excipient from cellulose to enhance the effectiveness of antibiotics and inhibit drug resistance. *CCS Chem*. **2026**, doi: 10.31635/ccschem.026.202608343.
15 Qiu, Y. J.; Zhang, D. C.; Long, M.; Zhou, Z. X.; Gao, C. D.; Ma, S.; Qin, J. F.; Chen, K. J.; Chen, C. J.; Zhao, Z.; Deng, H. B. Coassembly of hybrid microscale biomatter for robust, water-processable, and sustainable bioplastics. *Sci. Adv.* **2025**, *11*, 1596.
16 Wang, Y. R.; Ma, J. X.; Shao, C.; Yin, C. C.; Wang, Y. L.; Wang, J. F.; Zhang, J. M.; Wang, J. Z.; Zhang, J. Significant Increase of Carrier Mobilities for Efficient and Stable Solar Cells by Repairing Interfaces of Perovskite. *CCS Chem.* **2026**, *8*, 2387–2402.
17 Liu, S. L.; Zhang, Q.; Gou, S. H.; Zhang, L. L.; Wang, Z. G. Esterification of cellulose using carboxylic acid-based deep eutectic solvents to produce high-yield cellulose nanofibers. *Carbohyd. Polym.* **2021**, *251*, 117018.
18 Zhou, M.; Chen, D. Z.; Chen, Q. Q.; Chen, P.; Song, G. J.; Chang, C. Y. Reversible surface engineering of cellulose elementary fibrils: from ultralong nanocelluloses to advanced cellulosic materials. *Adv. Mater.* **2024**, *36*, 2312220.
19 Yang, X. P.; Abe, K.; Yano, H.; Wang, L. Multifunctional cellulosic materials prepared by a reactive DES based zero-waste system. *Nano Lett.* **2022**, *22*, 6128–6134.
20 Sirviö, J. A. Cationization of lignocellulosic fibers with betaine in deep eutectic solvent: facile route to charge stabilized cellulose and wood nanofibers. *Carbohyd. Polym.* **2018**, *198*, 34–40.
21 Yang, X.; Reid, M. S.; Olsén, P.; Berglund, L. A. Eco-friendly cellulose nanofibrils designed by nature: effects from preserving native state. *ACS Nano* **2020**, *14*, 724–735.
22 Yu, Y. Y.; Cheng, W. K.; Li, Y. L.; Wang, T.; Xia, Q. Q.; Liu, Y. Z.; Yu, H. P. Tailored one-pot lignocellulose fractionation to maximize biorefinery toward versatile xylochemicals and nanomaterials. *Green Chem.* **2022**, *24*, 3257–3268.
23 Shi, X. C.; Wang, Z. B.; Liu, S. Y.; Xia, Q. Q.; Liu, Y. Z.; Chen, W. S.; Yu, H. P.; Zhang, K. Scalable production of carboxylated cellulose nanofibres using a green and recyclable solvent. *Nat. Sustain.* **2024**, *7*, 315–325.
24 Haque, A. M. A.; Vanniappan, G.; Bayattork, M.; Zhang, Y.; Naebe, M. Green nanofibrillation of hemp cellulose *via* deep eutectic solvent and simple shear mixing: a response surface approach to process refinement. *ACS Sustainable Chem. Eng.* **2026**, *14*, 812–826.
25 Norizan, M. N.; Shazleen, S. S.; Alias, A. H.; Sabaruddin, F. A.; Asyraf, M. R. M.; Zainudin, E. S.; Abdullah, N.; Samsudin, M. S.; Kamarudin, S. H.; Norrrahim, M. N. F. Nanocellulose-based nanocomposites for sustainable applications: a review. *Nanomaterials* **2022**, *12*, 3483.
26 Wang, B.; Dai, H. Y.; Zhang, C. H.; Dong, Z. C.; Li, K.; Jiang, L. Nasal cavity inspired micro-nanostructured cone array tube for oil recovery in wastewater. *Adv. Mater. Interfaces* **2022**, *9*, 2102311.
27 Satam, C. C.; Irvin, C. W.; Coffey, C. J.; Geran, R. K.; Ibarra-Rivera, R.; Shofner, M. L.; Meredith, J. C. Controlling barrier and mechanical properties of cellulose nanocrystals by blending with chitin nanofibers.. *Biomacromolecules* **2020**, *21*, 545–555.
28 Ru, J.; Tong, C. C.; Chen, N.; Shan, P. J.; Zhao, X. K.; Liu, X. Y.; Chen, J. Z.; Li, Q.; Liu, X. H.; Zhao, Y. Morphological and property characteristics of surface-quaternized nanofibrillated cellulose derived from bamboo pulp.. *Cellulose* **2019**, *26*, 1683–1701.
29 Luo, J. Q.; Su, Y. Q.; Liu, J. G.; Li, Q. Oxygen and water vapor barrier properties of nanocellulose materials: a review. *Trans. China Pulp Pap*. **2019**, *34*, 61–70.